

## Article

# Characteristics of Biochar Obtained by Pyrolysis of Residual Forest Biomass at Different Process Scales

Márcia Santos , Ana Carolina Morim , Mariana Videira, Flávio Silva , Manuel Matos and Luís A. C. Tarelho \* 

Department of Environment and Planning, Centre for Environmental and Marine Studies (CESAM), University of Aveiro, 3810-193 Aveiro, Portugal; marciasantos@ua.pt (M.S.); carolinapedrosamorim@ua.pt (A.C.M.); mvideira99@ua.pt (M.V.); flavio.silva@ua.pt (F.S.); amatos@ua.pt (M.M.)

\* Correspondence: ltarelho@ua.pt

**Abstract:** In this work, the pyrolysis process and the characteristics of biochar produced using a bench-scale fixed-bed reactor and a prototype-scale auger reactor were studied. Residual forest biomass (RFB) from acacia, broom, gorse, and giant reed was used as feedstock. Besides information on pyrolysis characteristics of these specific biomass species from the Iberian Peninsula, new knowledge on the understanding of how results from small-scale reactors can be used to predict the behavior of higher-scale and continuous-operation reactors is offered. Batch pyrolysis was carried out using 40 g of biomass sample in a fixed-bed reactor with a heating rate of  $20\text{ }^{\circ}\text{C}\cdot\text{min}^{-1}$ , pyrolysis temperature of 450 and 550  $^{\circ}\text{C}$ , and a residence time of 30 min, while for the continuous process it was used a prototype of an auger reactor with continuous operation with a biomass flow rate up to 1 kg/h, with temperatures of 450 and 550  $^{\circ}\text{C}$ , and a solids residence time of 5 min. The biochar yield was in the range of 0.26 to 0.36 kg/kg biomass dry basis, being similar for both types of reactors and slightly lower when using the auger reactor. The proximate analysis of the biochar shows volatile matter in the range 0.10 to 0.27 kg/kg biochar dry basis, fixed carbon in the range 0.65 to 0.84 kg/kg biochar dry basis, and ash in the range 0.04 to 0.08 kg/kg biochar dry basis. The carbon, oxygen, and hydrogen content of the biochar was in the range of 0.71 to 0.81, 0.09 to 0.22, and 0.02 to 0.03 kg/kg biochar dry basis, respectively. The results show that the up-scaling of the reactor and regime of operation does not have an important influence on the yield and characteristics of the biochar produced. The biochar obtained in the two types of reactors has characteristics appropriate for environmental applications, such as an additive to improve soil properties. It is possible to see that the characteristics of the biochar are influenced by the type of biomass and the conditions and parameters of the process; therefore, it is of major importance to control and know of these conditions, especially when considering upscaling scenarios.

**Keywords:** biomass; pyrolysis; char; auger reactor; fixed-bed batch reactor



**Citation:** Santos, M.; Morim, A.C.; Videira, M.; Silva, F.; Matos, M.; Tarelho, L.A.C. Characteristics of Biochar Obtained by Pyrolysis of Residual Forest Biomass at Different Process Scales. *Energies* **2024**, *17*, 4861. <https://doi.org/10.3390/en17194861>

Academic Editors: Mingxin Xu and Xiaobin Qi

Received: 3 September 2024

Revised: 19 September 2024

Accepted: 26 September 2024

Published: 27 September 2024



**Copyright:** © 2024 by the authors. Licensee MDPI, Basel, Switzerland. This article is an open access article distributed under the terms and conditions of the Creative Commons Attribution (CC BY) license (<https://creativecommons.org/licenses/by/4.0/>).

## 1. Introduction

The use of biomass as an energy source plays an important role due to the added benefits, such as the reduction of greenhouse gas emissions and diversification in the supply of renewable energy, thus reducing the use of fossil fuels [1,2]. Among the existing biomass sources, the agro-residues, residual forest biomass, municipal solid waste, and food processing residues [3,4], have a twofold relevance; they need to be properly managed, and they can be used as a source of primary energy [3]. Residual forest biomass is currently one of the most popular sources of biomass for bioenergy [4] and is generated in large quantities from forest maintenance operations, often carried out to prevent wildfires. In the case of Portugal, there is great potential for the use of this residual forest biomass (RFB), as approximately 90% of the country's territory is composed of forests, shrubs, pastures, and agricultural land [5]. Furthermore, using RFB as an energy source also contributes to the prevention of wildfires since it includes vegetation types with flammable characteristics [4].

The issue of wildfires affects countries such as Portugal and Spain, which are fire-prone due to their dry summers and forests containing flammable tree and shrubland species. In Portugal, wildfires are often associated with the proliferation of residual forest biomass, which promotes the accumulation of fuel. In addition to the negative impacts on the rural and forestry economies, fires are also a driver of desertification and the degradation of soil quality and fertility. In Portugal, wildfires have affected 2.2% (annual average) of the total land area occupied by forests, woodlands, grasslands, and scrublands over the past decade [6]. From 2019 to 2023, there were more than 45,000 rural fires, burning a total area of approximately 280,000 hectares [7]. When expanding this topic to the European Union, the most recent Annual Fire Reports from the European Forest Fire Information System indicate that 2022 was the second worst year in terms of burned area due to wildfires in the EU, with nearly 900,000 hectares of natural lands affected by fire, causing a significant impact on the EU's biodiversity reservoir [8].

There are several options for using biomass as an energy source, which have variable costs and applicability [9]. Specifically in the case of RFB, there are strong limitations depending on the composition of the material, namely the concentration and composition of inorganics (including elements such as K, Na, and Cl) that are often related to high-temperature operational problems in thermochemical processes such as combustion and gasification, for example [10,11].

However, pyrolysis is a thermochemical process that can be used for those low-grade and problematic types of RFB. During pyrolysis, the biomass is subjected to a coupled set of thermal and chemical processes that causes the release of volatile matter from the biomass to the gas phase in an O<sub>2</sub>-free environment, generating a solid product rich in carbon called biochar, where most of the inorganic constituents of the raw material are incorporated [12,13]. The European Biochar Certificate [14] defines biochar as “a porous, carbonaceous material that is produced by pyrolysis of biomass and is applied in such a way that the contained carbon remains stored as a long-term C sink or replaces fossil carbon in industrial manufacturing”. The most common application of biochar is its use as a soil corrective, due to its characteristics that potentiate nutrient recycling and increase soil water holding capacity, thus reducing the consumption of inorganic fertilizers and greenhouse gas emissions, but also contributing to carbon sequestration [15–17]. Furthermore, because it has oxygenated groups on its surface, biochar can also be applied as an adsorbent for organic contaminants and heavy metals in soil and water [18,19]. Because it is a low-cost, sustainable material with good availability, high electronic conductivity, corrosion resistance, and a large surface area, it is also used as fuel for fuel cells [20], as a precursor for obtaining activated carbon [21], and as a catalyst in processes for syngas cleaning and biodiesel production, for example [22,23].

The characteristics and yields of the products obtained in the pyrolysis process, namely biochar, bio-oil, and gas, are dependent on the operating conditions (for example, process temperature, heating rate, and residence time), the type of biomass, and the type of reactor used in the process [13,15,24]. For this reason, it is important to know the influence of these factors and how they can be changed to optimize the pyrolysis process.

Regarding the type of reactor, most research studies of the properties and yields of pyrolysis products have been carried out in fixed-bed batch reactors, which work on smaller scales, due to their ease of operation and maintenance [15,25]. Even on larger scales, due to its low cost and simplicity, archaic batch-type pyrolysis furnace systems with low energy efficiency, such as brick kilns, retorts, and hot tail kilns, are still the most common for charcoal production from biomass. However, they have a high environmental impact, as pyrolysis gases are typically released into the atmosphere without any treatment nor energetic valorization [15,26]. Auger reactors with burning pyrolysis gases downstream have been suggested as one of the most suitable alternatives for carbonization processes, and in particular for biochar production, as long as the process parameters and characteristics of the biomass used are known, since these factors can change not only the characteristics and yield of the products formed but also the amount of thermal energy that will be produced

from the combustion of the pyrolysis gases [27,28]. This type of reactor has the advantage of being easy to operate and also allowing the biomass residence time in the pyrolysis zone to be easily controlled and modified by the screw rotation frequency [29], making it a promising alternative for working with raw materials with heterogeneous characteristics, such as RFB. Additionally, the auger reactor can facilitate adequate mixing of the feedstock particles, improving contact between these particles and the heated reactor wall, and exposing them to increased uniformity when thermal conditions are applied during the pyrolysis process [30].

In order to develop pyrolysis technology at an industrial level and promote the supply of sustainable pyrolysis products, one must know and understand the influence of scaling up the process on product yield and quality. Del Pozo et al. [25] analyzed the bio-oil and biochar produced in an auger reactor at two scales ( $0.3$  and  $15 \text{ kg}\cdot\text{h}^{-1}$ ) by pyrolysis of biomass derived from solid residues from coffee roasting, winemaking and olive oil production processes and found no major differences in solid products (biochar) when temperature and residence time were fixed. Meng et al. [31] used a fixed-bed tubular reactor and an auger reactor to compare the effect of scaling but focused the study on the properties and environmental risks of potentially toxic elements in biochar obtained from swine manure. Prithiraj and Kauchali [32] developed an industrial-scale reactor with a capacity of 1200 L; however, they worked with refinery residue and a fixed-bed reactor. For these conditions, they found that if the sample volume is too large and there is no internal mechanism to stir the feedstock, a partial pyrolysis of the material may occur. Park et al. [33] employed two types of pyrolysis processes to obtain biochar and bio-oil from biomass harvested from heavy-metal-contaminated areas: batch-wise one-stage pyrolysis and continuous two-stage pyrolysis (auger and fluidized bed reactors). The study concluded that the products obtained had different characteristics depending on the process characteristics. However, in that work, the objective was different: the two-stage process was designed to separately produce a cellulose- and hemicellulose-derived product (in the auger reactor at  $300 \text{ }^\circ\text{C}$ ) and a lignin-derived product (in the fluidized bed reactor at  $550 \text{ }^\circ\text{C}$ ). The process used 400 g of biomass over 1 h, while the fixed-bed reactor pyrolyzed 100 g of biomass at  $550 \text{ }^\circ\text{C}$ . Salgado et al. [27] studied the production of biochar from palm oil residual biomass using a prototype of a modular auger reactor. They found that, with a biomass feed rate of  $30 \text{ kg}\cdot\text{h}^{-1}$ , the reactor was able to be thermally sustained by the energy generated from the combustion of pyrolysis vapors, producing biochar with chemical characteristics in accordance with European guidelines. This type of study is highly relevant in the context of scaling up and expanding the global use of pyrolysis.

Studies comparing the influence of different scales of reactors for RFB pyrolysis are still scarce, which justifies the importance of this knowledge in order to understand how results from small-scale, and often batch-operated, laboratorial reactors can be used to infer about properties and yields of pyrolysis products from specific biomasses in the decision support for medium- to large-scale design of pyrolysis systems.

In this work, a comparative analysis is made of the characteristics and yield of the biochar produced from the pyrolysis of four different residual forest biomasses, namely, acacia, gorse, broom, and giant reed, using two different experimental installations: a fixed-bed batch reactor and an auger reactor with continuous operation. The reactors work on different process scales, with the fixed-bed batch reactor using around 40 g of biomass per batch, while the continuous auger reactor works with approximately  $1 \text{ kg}\cdot\text{h}^{-1}$  of biomass. The influence of process temperature on the biochar yield and properties is also analyzed.

## 2. Materials and Methods

In this chapter, the experimental facilities developed for the comparative study of the process scales are described, as well as the methodologies used for characterization of the biomass and biochar.

### 2.1. Experimental Facility

A schematic representation of the experimental bench-scale pyrolysis system operated in batch mode is shown in Figure 1. The fixed-bed reactor consists of a quartz tube 33 mm in external diameter, 30 mm in internal diameter, and 650 mm in length (the biomass batch occupies 370 mm in length). This quartz tube is heated by a tubular furnace, which operates according to a control and data acquisition system, thus allowing the definition of the pyrolysis temperature, the heating rate, and the process time. The temperatures throughout the experiments were monitored by four K-type thermocouples, located at different zones of the reactor, and recorded by a datalogger. One thermocouple was inserted in the batch of biomass (T4 in Figure 1) and was used to control the temperature and heating rate, and the other three thermocouples were located at three locations at the outside wall of the quartz tube.

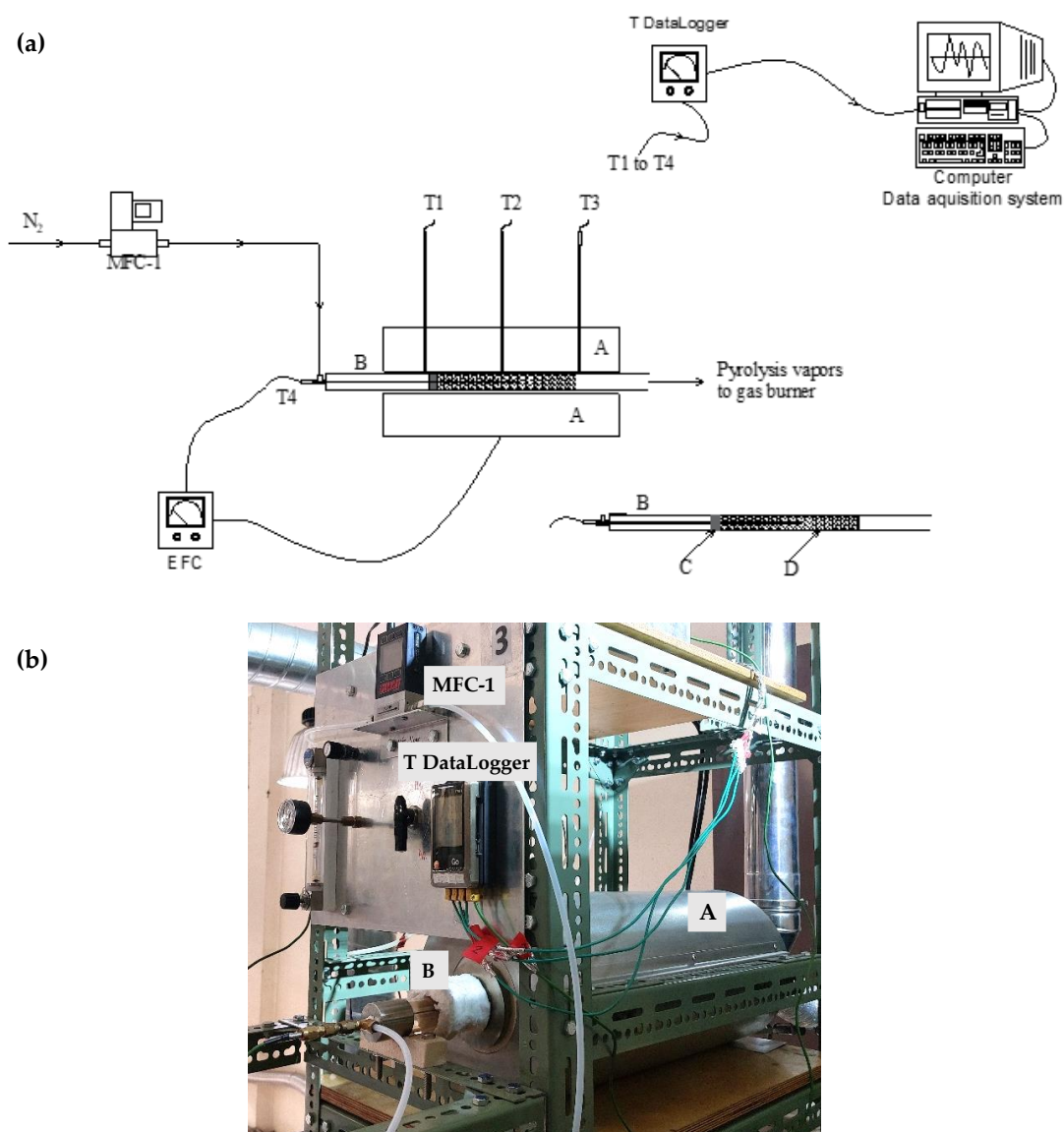


**Figure 1.** (a) Schematic representation and (b) picture of the experimental facility of the fixed-bed batch reactor used in pyrolysis experiments, with a (A) tubular electric furnace, (B) quartz tube, (C) ceramic fiber, (D) biomass/biochar, (EFC) electric furnace controller, and a (MFC-1) gas mass flow controller (T1 to T4) thermocouples.

For each experiment in this reactor, a sample of approximately 40 g of biomass is loaded into the quartz tube, which is taken inside the furnace under an inert atmosphere controlled

by the injection of  $N_2$  ( $0.150 \text{ L}_{\text{NTP}} \cdot \text{min}^{-1}$ , NPT means standard pressure ( $1 \times 10^5 \text{ Pa}$ ) and temperature ( $273 \text{ K}$ )). Process conditions included two setpoint temperatures ( $450 \text{ }^\circ\text{C}$  and  $550 \text{ }^\circ\text{C}$ ), a heating rate of  $20 \text{ }^\circ\text{C} \cdot \text{min}^{-1}$ , and a processing time of  $30 \text{ min}$  after reaching the desired temperature setpoint. After completion of the required process time, the quartz tube is removed from the furnace and cooled at room temperature. The biochar obtained is weighted and its yield calculated through Equation (1).

$$Y_{BC} = \frac{m_{BC}}{m_B}, \quad (1)$$

where  $Y_{BC}$  is biochar yield ( $\text{kg biochar}/\text{kg biomass dry basis}$ );  $m_{BC}$  is the biochar mass in dry basis ( $\text{kg}$ ); and  $m_B$  is the biomass mass in dry basis ( $\text{kg}$ ).

The continuous pyrolysis process was carried out in an auger reactor with the layout configuration shown in Figure 2. The reactor is made of refractory steel 253MA, as is a circular section tube with a screw-feeder operating inside (C in Figure 2), with an overall length of  $1.8 \text{ m}$  and  $0.054 \text{ m}$  internal diameter. The raw material is fed into the silo and is loaded into the pyrolysis section by a screw that rotates at a controlled rotation frequency, thus allowing the definition and control of the residence time of the biomass/char in the high temperature region (electric furnace, C in Figure 2). The electric furnace is heated at a predefined temperature, controlled through a control and data acquisition system. After passing through the pyrolysis section, the biochar is collected in a discharge silo (I in Figure 2), while the gases generated in the process are continuously burned in a combustion chamber (located after G in Figure 2). The reactive system has a continuous injection of  $N_2$  in the feed silo and in the biochar discharge silo of  $1.0$  and  $0.5 \text{ L}_{\text{NTP}} \cdot \text{min}^{-1}$ , respectively.

(a)

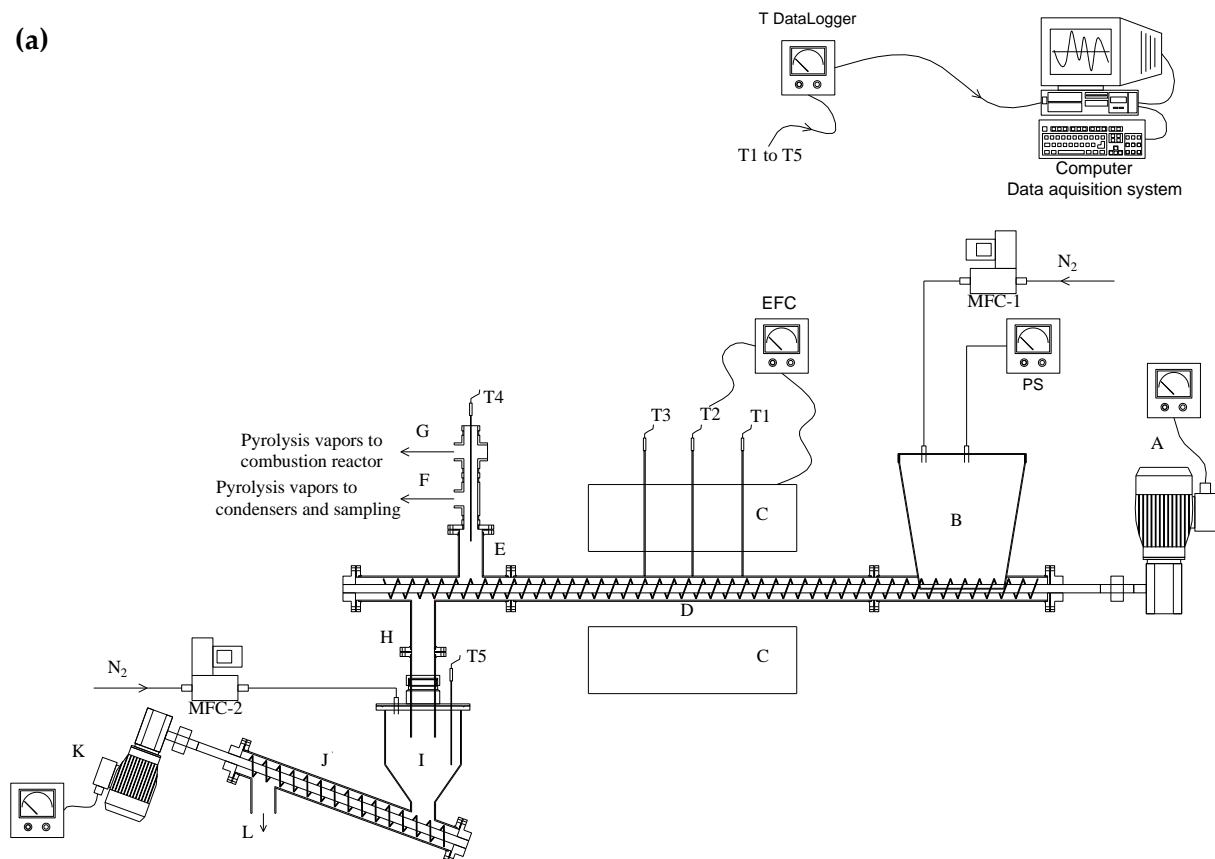
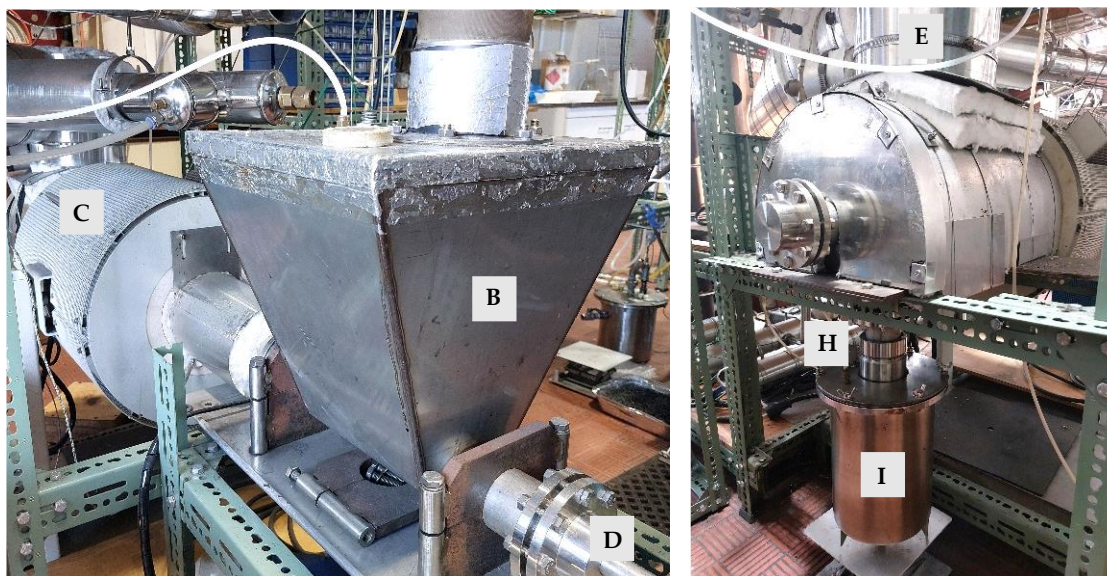


Figure 2. Cont.

(b)



**Figure 2.** (a) Schematic representation and (b) picture of the experimental facility of the auger reactor, where (A) electric motor and speed controller, (B) biomass silo, (C) electric furnace, (D) auger reactor tube and screw feeder, (E) pyrolysis vapors exit, (F) pyrolysis vapors exit to condensers and sampling, (G) pyrolysis vapors exit to combustion reactor, (H) biochar discharge port, (I) biochar discharge silo, (J) biochar discharge screw-feeder, (L) biochar discharge, (K) electric motor and speed controller, (EFC) electric furnace controller, (PS) pressure sensor, (MFC-1 to 2) gas mass flow controllers, and (T1 to T5) thermocouples.

In this reactor, each experiment involved the processing of biomass with a mass flow rate in the range of  $0.2 \text{ kg}\cdot\text{h}^{-1}$  to  $0.9 \text{ kg}\cdot\text{h}^{-1}$ . The pyrolysis temperature, as defined in the furnace region (T2 in Figure 2), was  $450 \text{ }^{\circ}\text{C}$  and  $550 \text{ }^{\circ}\text{C}$ , and the biomass/char residence time in the pyrolysis zone was 5 min, corresponding to a screw rotation speed of 3 rpm. After passing all the biomass through the reactor, the collected biochar has its mass determined and its yield calculated following Equation (1).

## 2.2. Biomass

Biomass samples used were collected in forest maintenance operations for wildfire prevention, conducted in the central region of Portugal, characterized by its typical temperate Mediterranean climate, specifically in the districts of Aveiro, Viseu, and Coimbra, during the first half of 2023. The biomass species included are shown in Table 1.

**Table 1.** Usual and scientific nomenclature of different biomasses.

Common Name	Scientific Name
Acacia	<i>Acacia longifolia</i>
Gorse	<i>Ulex europaeus</i>
Broom	<i>Cytisus striatus</i>
Giant reed	<i>Arundo donax</i>

The raw biomass samples were air dried, chipped, and sieved to achieve the appropriate granulometry for the pyrolysis experiment, and typical particle size below 10 mm. The biomass samples were then characterized for proximate analysis (determination of the volatile matter, ash, fixed carbon, and moisture), ultimate analysis (determination of carbon, hydrogen, oxygen, nitrogen, and sulfur), heating value, and bulk density. For proximate analysis, the procedure was in accordance with the following standards: "CEN/TS 14774-

3:2004—Solid biofuels—Methods for the determination of moisture content” [34]; “CEN/TS 15148:2005—Solid biofuels—Method for the determination of the content of volatile matter” [35]; and “CEN/TS 14775:2004—Solid biofuels—Method for the determination of ash content” [36]. The fixed carbon was calculated using Equation (2).

$$w_{FC} = 1 - (w_{Ash} + w_{VM}), \quad (2)$$

where  $w_{FC}$  is mass fraction of fixed carbon (kg/kg biomass dry basis),  $w_{Ash}$  is mass fraction of ash (kg/kg biomass dry basis), and  $w_{VM}$  is mass fraction of volatile matter (kg/kg biomass dry basis).

The concentration of carbon, hydrogen, nitrogen and sulfur were determined through an element analyzer (Model EA1108, Fison Instruments Ltd., Glasgow, United Kingdom). The oxygen concentration was determined by the difference using Equation (3).

$$w_O = 1 - (w_C + w_H + w_N + w_S + w_{Ash}), \quad (3)$$

where  $w_O$  is mass fraction of oxygen (kg/kg biomass dry basis),  $w_C$  is mass fraction of carbon (kg/kg biomass dry basis),  $w_H$  is mass fraction of hydrogen (kg/kg biomass dry basis),  $w_N$  is mass fraction of nitrogen (kg/kg biomass dry basis),  $w_S$  is mass fraction of sulfur (kg/kg biomass dry basis), and  $w_{Ash}$  is mass fraction of ash (kg/kg biomass dry basis).

The higher heating value (HHV) of the dry biomass samples was determined using a calorimetric pump, model CAL2K-ECO (DDS Calorimeters, Randburg, South Africa), following standard “DIN 51,900—Determining the gross calorific value of solid and liquid fuels using the bomb calorimeter, and calculation of net calorific value” [37]. The lower heating value (LHV) was determined by calculation, through Equation (4).

$$LHV = HHV - L_v \times w_H \times \frac{M_{H_2O}}{M_{H_2}}, \quad (4)$$

where  $LHV$  is lower heating value ( $\text{MJ}\cdot\text{kg}^{-1}$ );  $HHV$  is higher heating value ( $\text{MJ}\cdot\text{kg}^{-1}$ );  $L_v$  is latent heat of vaporization of the water ( $\text{MJ}\cdot\text{kg}_{\text{H}_2\text{O}}^{-1}$ );  $w_H$  is mass fraction of hydrogen (kg/kg biomass dry basis);  $M_{\text{H}_2\text{O}}$  is molar mass of water ( $\text{g}\cdot\text{mol}^{-1}$ ); and  $M_{\text{H}_2}$  is molar mass of hydrogen ( $\text{H}_2$ ) ( $\text{g}\cdot\text{mol}^{-1}$ ).

The bulk density of the biomass samples was obtained through the relation between their mass and the respective occupied volumes. And in was determined following the standard “SIS-CEN/TS 15103:2006—Solid biofuels—Methods for the determination of bulk density” [38].

The processed and characterized biomass samples were then used in the pyrolysis experiments in the two types of reactors and respective process conditions.

### 2.3. Biochar

In order to compare the biochar yield and characteristics obtained in the two types of reactors, the biochar samples were characterized for proximate and ultimate analysis, following the same methods used for biomass (Section 2.2). From the ultimate analysis, it was calculated the molar ratios O/C and H/C, important parameters that indicate the degree of carbonization and, consequently, the biochar stability.

In addition, the biochar produced in an auger reactor was also characterized for other parameters. Scanning Electron Microscopy (SEM) was used to obtain images of the surface structure of the biochar samples at  $1000\times$  magnification. For this, equipment Hitachi SU70 was used, with a 15 kV voltage and the samples without coating. The higher and lower heating values follow the same procedure as for biomass (Section 2.2). The pH using the standard “ISO 10390:2021 Soil, treated biowaste and sludge—Determination of pH” [39]. The electrical conductivity following the recommendations of the European Biochar Certificate [14], which suggests a method in analogy to “ISO 11265:1994 Soil quality—Determination of the specific electrical conductivity” [40]. The bulk density, the

apparent density, the true density, and the porosity based on the apparent and the true density values; for this, an adapted method was used [41], based on the pycnometer technique, using water as a displacement agent. This method is based on some standards and also on other studies [42–45]. The biochar samples obtained in an auger reactor were also characterized for polycyclic aromatic hydrocarbons (PAHs) and polychlorinated biphenyls (PCBs) following standard “CZ\_SOP\_D06\_03\_161 Determination of semi volatile organic compounds by gas chromatography method with MS or MS/MS detection and calculation of semi volatile organic compounds sums from measured values” [46,47].

### 3. Results and Discussion

The biomass and biochar characterization results are presented in this section. It is also made a comparison between the biochar yield obtained in the two different reactors and some of their characteristics.

#### 3.1. Biomass

After drying and chipping processes, the biomass samples (Figure 3) were characterized, and the results for proximate and ultimate analysis are shown in Figure 4. All samples had moisture content between 0.08 and 0.11 kg H<sub>2</sub>O/kg biomass. The volatile matter content in the biomass was in the range of 0.75 to 0.80 kg/kg biomass dry basis, and broom was the biomass with the highest content. The fixed carbon content in the biomass ranged from 0.18 to 0.23 kg/kg biomass dry basis, with acacia showing the higher value and broom the lower value. Regarding the ash content, giant reed presented the maximum value of 0.025 kg/kg biomass dry basis, while the other biomasses presented values in the range of 0.012 to 0.022 kg/kg biomass dry basis. The ash content of the raw biomass influences the ash content of the formed biochar, in addition to influencing the pH of the final product since many alkaline ions are present in the ash [48].



**Figure 3.** Macroscopic view of the biomass samples used in the pyrolysis experiments: (A) acacia, (B) gorse, (C) broom, and (D) giant reed.

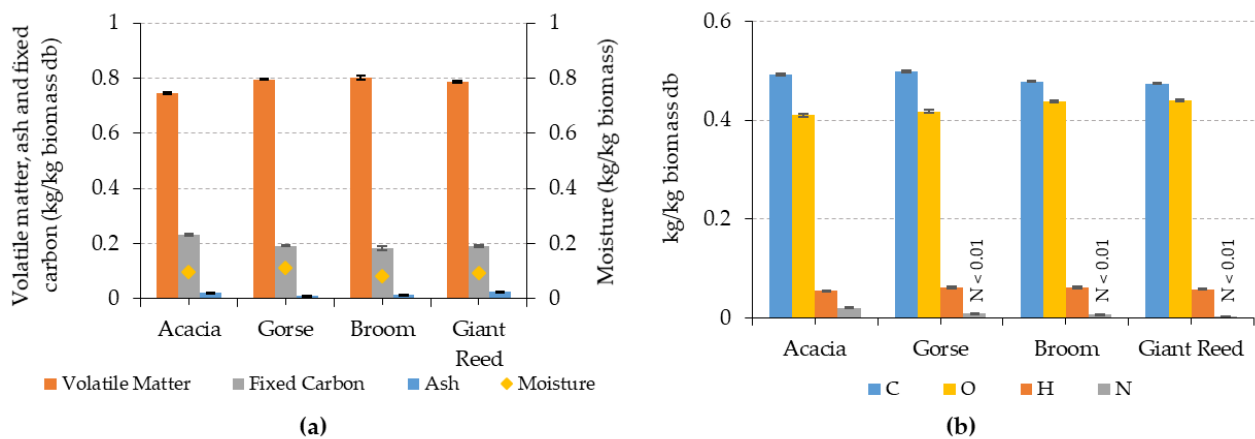


**Figure 4.** (a) Proximate and (b) ultimate analysis of distinct biomass types. Sulfur concentration is not shown because it was below 100 ppm wt.; the detection limit of the analytical method used.

The carbon concentration in the biomass samples is in the range of 0.47 to 0.50 kg/kg biomass dry basis, with the highest value found for gorse. Gorse and broom are the biomasses with the highest hydrogen concentration (0.062 kg/kg biomass dry basis), while acacia is the biomass with the highest nitrogen concentration (0.021 kg/kg biomass dry basis). With regard to oxygen, its concentration in the biomass samples was in the range of 0.41 to 0.44 kg/kg biomass dry basis. The sulfur concentration in the biomasses was below 100 ppm, corresponding to the detection limit of the analytical method used.

In Table 2, it is shown the higher heating value (HHV) and lower heating value (LHV) for the studied biomasses, and in Figure 5, the relation between heating value and the concentration of carbon, oxygen, and hydrogen in the biomass. Giant reed is the biomass with the lowest HHV,  $17 \text{ MJ}\cdot\text{kg}^{-1}$ , while the other samples showed values around  $19 \text{ MJ}\cdot\text{kg}^{-1}$ . This result reflects the composition of the biomass samples because giant reed has a higher ash and oxygen concentration and a lower carbon and hydrogen concentration. It is known the positive correlations between the heating value and the concentrations of carbon and hydrogen and the negative correlation between the heating value and the ash and oxygen concentration [49].

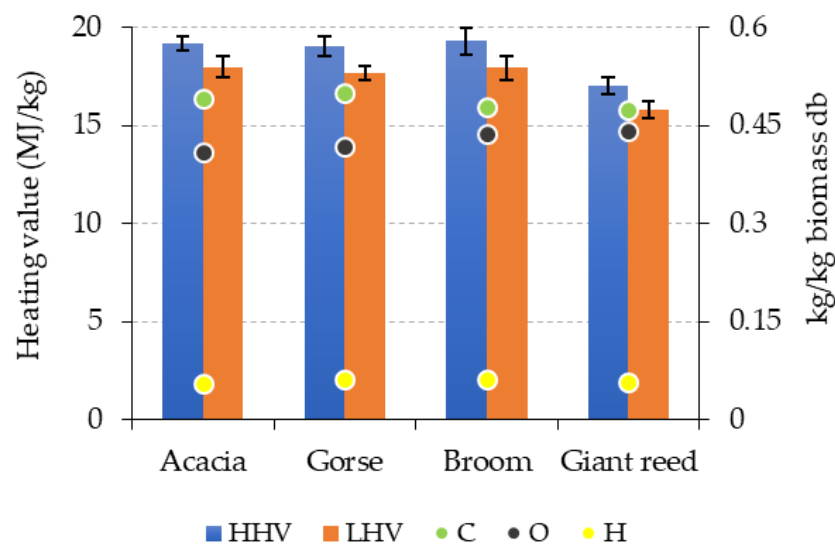


**Figure 5.** Higher heating value (HHV) and lower heating value (LHV) and concentration of carbon, hydrogen, and oxygen of the distinct biomass types (dry basis).

**Table 2.** Higher heating value (HHV) and lower heating value (LHV) of the biomass samples (dry basis).

Sample	HHV (MJ·kg <sup>-1</sup> )	LHV (MJ·kg <sup>-1</sup> )
Acacia	19.19 ± 0.52	17.99 ± 0.52
Gorse	19.03 ± 0.38	17.67 ± 0.38
Broom	19.29 ± 0.61	17.93 ± 0.61
Giant reed	17.05 ± 0.45	15.79 ± 0.45

In Table 3, it is shown the bulk density of the chipped biomass samples (Figure 3). This parameter is not intrinsic to the material but depends on the size, shape, and compaction of its particles [50]. The bulk density is important to know, as it impacts the material's handling, transport, and application.

**Table 3.** Bulk density of the chipped biomass samples.

Sample	Bulk Density (kg·m <sup>-3</sup> )
Acacia	120.05 ± 12.65
Gorse	86.78 ± 3.06
Broom	101.50 ± 3.96
Giant reed	177.03 ± 5.17

### 3.2. Biochar Yield

The biochar obtained from the two different experimental facilities was compared for yield in the pyrolysis process and its characteristics (proximate and ultimate analysis).

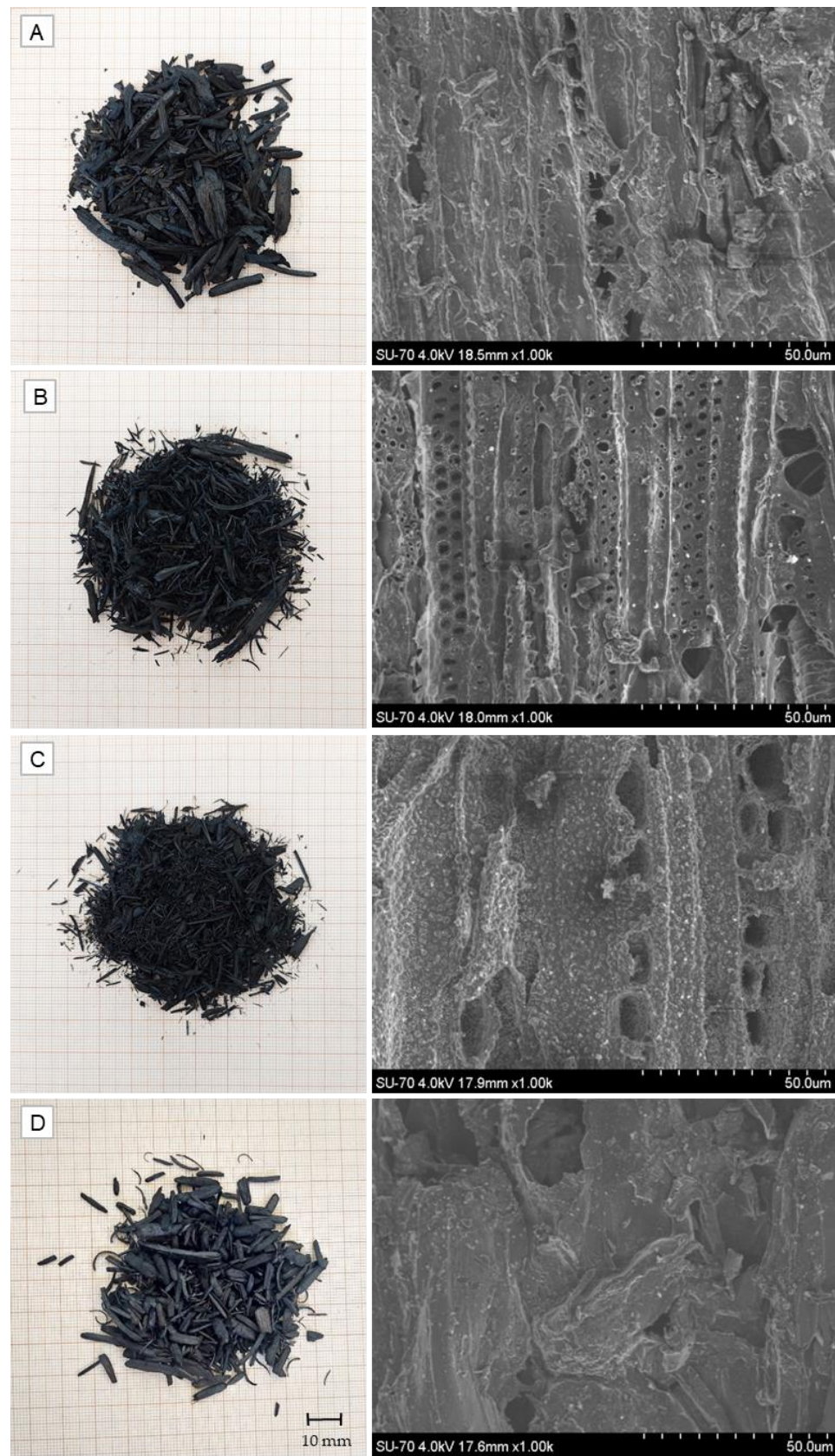
An example of the macroscopic aspect and surface morphology of the biochar obtained in the auger reactor at 550 °C is shown in Figure 6. The macroscopic aspect of the biochar obtained at 450 °C and 550 °C is very similar. The SEM images refer to a longitudinal particle at 1000× magnification. It is possible to observe the presence of some pores on the surface of the biochar obtained from acacia, gorse, and broom, while the biochar from reed exhibits a smoother surface in the obtained image.

Figure 7 shows the biochar yield in the pyrolysis processes carried out at 450 °C and 550 °C for the different biomasses and using the two reactor types.

For pyrolysis in the auger reactor, with a solids residence time of 5 min, the biochar yield was in the range of 0.28 to 0.33 kg/kg biomass dry basis and 0.26 to 0.29 kg/kg biomass dry basis for temperatures of 450 and 550 °C, respectively.

For pyrolysis in the fixed-bed batch reactor, with a heating rate of 20 °C·min<sup>-1</sup> and a solids residence time of 30 min after reaching the process temperature, the yield of biochar ranged from 0.30 to 0.36 kg/kg biomass dry basis and 0.28 to 0.31 kg/kg biomass dry basis for temperatures of 450 °C and 550 °C, respectively.

The results show that biochar yield decreases when the process temperature is higher, and this is explained by the higher thermochemical decomposition of the parent biomass at the higher temperatures, causing a higher release of volatile materials during pyrolysis. Comparing the two types of reactors, it is observed that for the same process temperature the biochar yield is in a similar range, and in some conditions the biochar yield is higher in the fixed-bed reactor and in others is higher in the auger reactor, without revealing a well-defined trend. For example, for gorse and giant reed, the biochar yield is always higher in the batch-operated reactor, whereas for broom, the biochar yield is slightly higher in the auger reactor. For acacia, there is an overlapping effect of temperature on the biochar yield, with lower temperatures promoting a higher biochar yield in the auger reactor, and the reverse is observed for the higher temperature. Nevertheless, considering biochar yield, it is observed that the small-scale batch-operated reactor provides a suitable indication of that parameter, and thus it is useful information to support the scale-up of pyrolysis processes for biochar production.



**Figure 6.** Macroscopic aspect and SEM images of the biochar obtained by pyrolysis in the auger reactor, at 550 °C and 5 min of residence time: (A) acacia, (B) gorse, (C) broom, and (D) giant reed. SEM images at 1000× magnification.

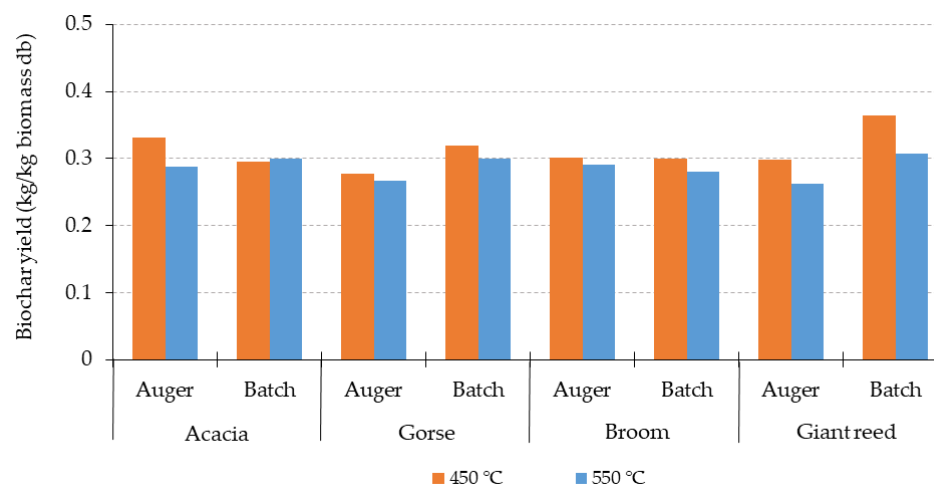


**Figure 7.** Biochar yield (kg/kg biomass dry basis) as a function of biomass type, process temperature and reactor type.

The influence of temperature on biochar yield has been discussed in numerous other studies. Lin et al. [51] and Silveira et al. [52] investigated the thermal degradation of wood during mild pyrolysis and concluded that the solid product yield was lower at higher temperatures. Yang et al. [53] established that biomass with a higher ash content produced biochar with a lower yield; they also observed that biochar yield decreased with increasing temperature. The comparison between two-stage pyrolysis (auger and fluidized bed reactors) and one-stage pyrolysis (fixed-bed reactor) was conducted by Park et al. [33], who found that the biochar yield from one-stage pyrolysis was higher than that from two-stage pyrolysis. This is attributed to the slow heating rate in the fixed-bed reactor, which favors biochar production.

### 3.3. Biochar Characteristics

#### 3.3.1. Proximate Analysis

In order to compare the influence of the type of reactor and process scale-up on the characteristics of the biochar produced, in Figure 8 are shown the results of proximate and ultimate analysis of the biochar samples obtained.

For the biochar produced from pyrolysis of the four biomass types in the auger reactor, at 450 °C, the volatile matter was in the range of 0.23 to 0.27 kg/kg of biochar dry basis, the ash was in the range of 0.04 to 0.07 kg/kg of biochar dry basis, and the fixed carbon was in the range of 0.65 to 0.71 kg/kg of biochar dry basis for the four different biomasses. For the temperature of 550 °C, the volatile matter was in range 0.16 to 0.19 kg/kg of biochar dry basis, the ash was in range 0.04 to 0.08 kg/kg of biochar dry basis, and the fixed carbon was in range 0.75 to 0.77 kg/kg of biochar dry basis for the four different biomasses.

The biochar obtained from pyrolysis of the four biomass types in the fixed-bed batch reactor at 450 °C has volatile matter from 0.20 to 0.24 kg/kg of biochar dry basis, ash from 0.04 to 0.06 kg/kg of biochar dry basis, and fixed carbon from 0.71 to 0.74 kg/kg of biochar dry basis. For the temperature of 550 °C, the volatile matter was from 0.10 to 0.16 kg/kg of biochar dry basis, the ash was in range 0.05 to 0.08 kg/kg of biochar dry basis, and the fixed carbon was in range 0.77 to 0.84 kg/kg biochar dry basis.

From Figure 8, it can be observed that higher temperatures promote the formation of biochar with lower volatile matter concentration and higher fixed carbon concentration. This effect of pyrolysis temperature has also been observed in other studies [54,55].

For both types of reactors and for the operating conditions tested, the fixed carbon is above 0.65 kg/kg of biochar dry basis and up to 0.84 kg/kg biochar dry basis. Also, the volatile matter concentration in the biochar is below 0.27 kg/kg of biochar dry basis, reflecting a more stable biochar material when compared to the parent biomass.

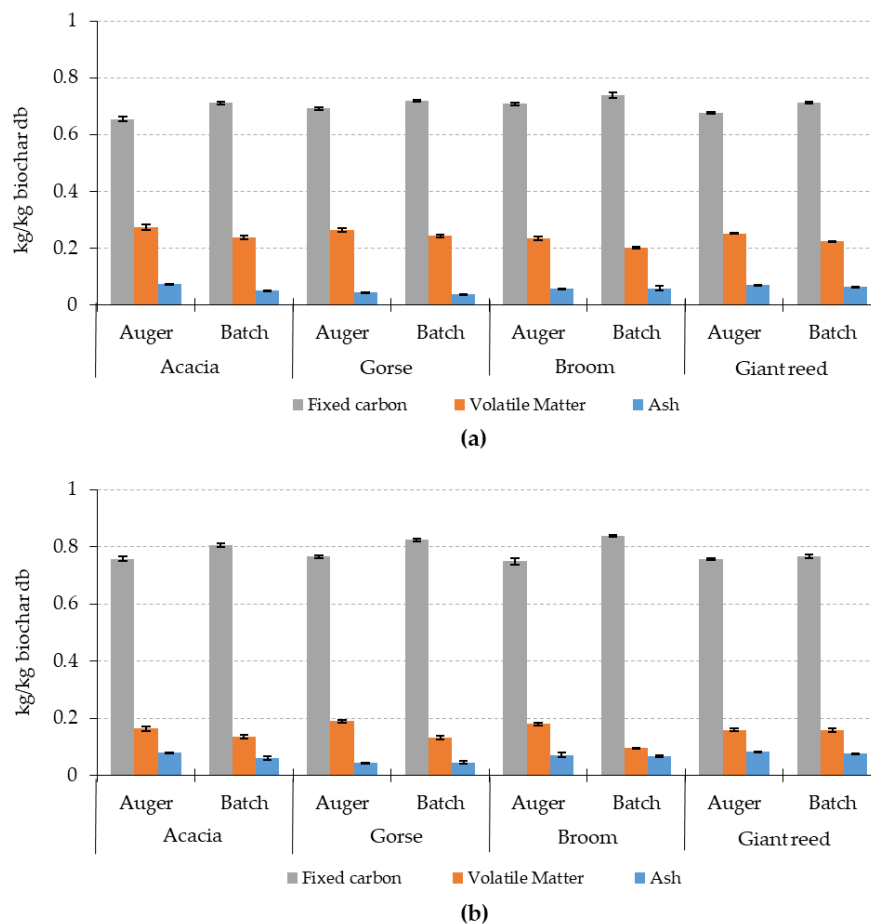


**Figure 8.** Volatile matter, fixed carbon and ash content of biochar produced from pyrolysis of distinct biomass and process temperature, in both reactors, at (a) 450 °C and (b) 550 °C.

It is observed that biochar produced in the auger reactor has lower fixed carbon content and higher ash and volatile matter content when compared to biochar from the batch-operated small-scale reactor. The higher volatile matter content of the biochar from the auger reactor can be explained as a result of a lower residence time of the biochar at the process temperature; in the auger reactor the solids residence time is 5 min in the high temperature region, whereas in the batch-operated reactor is 30 min (plus the time of the heating up to the defined process temperature), so it is expected a higher degree of thermal decomposition of the biomass in the batch-operated reactor and thus a corresponding lower volatile matter concentration in the biochar.

### 3.3.2. Ultimate Analysis

Figure 9 shows the ultimate analysis (CHNS) for the biochar produced in both reactors at the two temperatures studied. The pyrolysis process at 450 °C produced biochar with concentrations of carbon in the range of 0.71 to 0.75 kg/kg biochar dry basis, oxygen in the range of 0.14 to 0.22 kg/kg biochar dry basis, hydrogen in the range of 0.02 to 0.03 kg/kg biochar dry basis, and nitrogen in the range of 0.004 to 0.02 kg/kg biochar dry basis. At the temperature of 550 °C, the biochar obtained has a concentration of carbon in the range of 0.76 to 0.81 kg/kg biochar dry basis, oxygen in the range of 0.09 to 0.19 kg/kg biochar dry basis, hydrogen in the range of 0.02 to 0.03 kg/kg biochar dry basis, and nitrogen in the range of 0.005 to 0.02 kg/kg biochar dry basis. Thus, the increase in process temperature promoted the increase in the concentration of carbon and a decrease in the concentration of oxygen; there is a minor influence of temperature on the concentration of hydrogen and nitrogen. For both types of reactors and for the operating temperatures tested, the carbon concentration in the biochar is always higher than 0.71 kg/kg of biochar dry basis and up

to 0.81 kg/kg biochar dry basis. The nitrogen concentration in the biochar is very low, and below 0.02 kg/kg biochar dry basis.

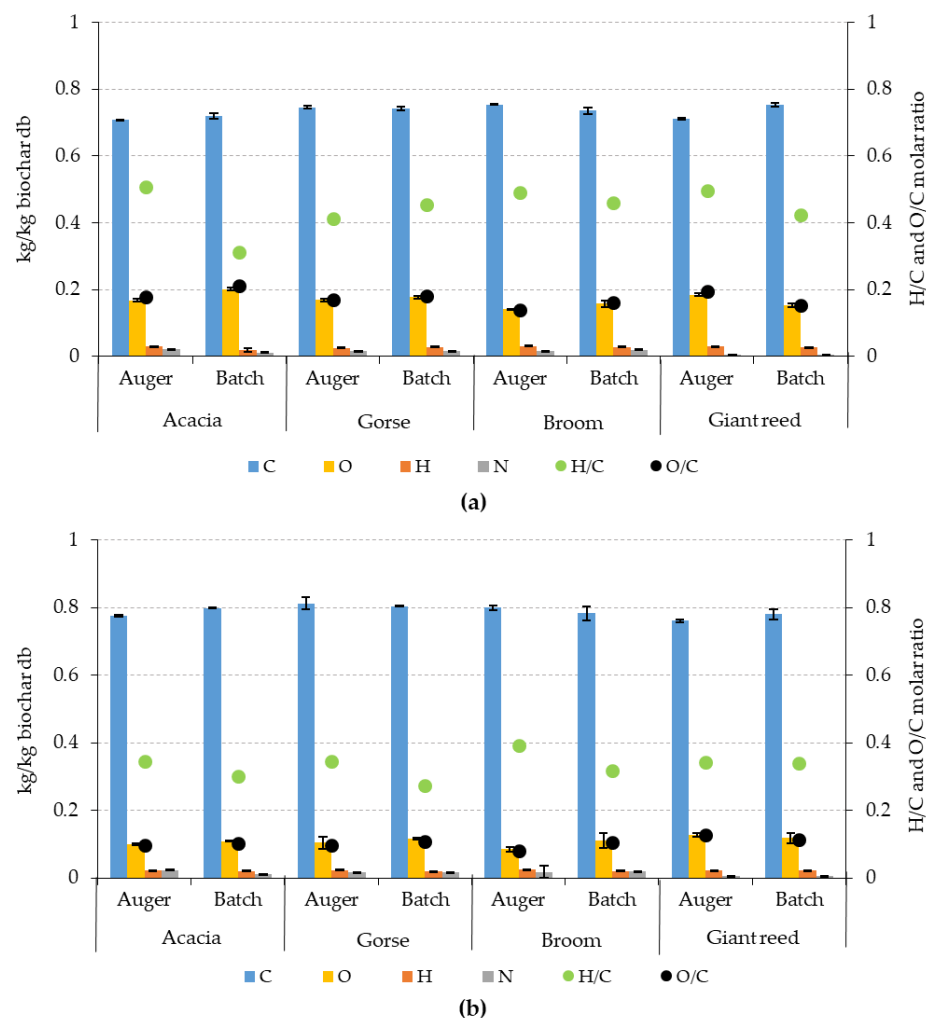


**Figure 9.** Elemental (CHNO) composition, H/C and O/C molar ratios for the biochar obtained from pyrolysis of distinct biomasses and process temperature, for both reactors, at (a) 450 °C and (b) 550 °C. Molar ratios were calculated on a dry basis. Sulfur concentration is not shown because it is below the detection limit (100 ppm wt.) of the method of analysis.

The effect of pyrolysis temperature on the elemental analysis of biochar showed the same trend in other studies. Qian et al. [54] characterized biochar obtained from different biomass species and observed an increase in carbon content and a decrease in hydrogen and oxygen content as the pyrolysis temperature increased. This same effect was observed by Toczydlowski et al. [55], who characterized biochar produced from two woody feedstocks at 350 °C and 450 °C.

There is not a clear trend for the influence of the type of reactor on the concentration of carbon and oxygen, and also for hydrogen and nitrogen in the biochar, for the two temperatures tested. For example, for acacia and giant reed pyrolysis, at both temperatures, it is observed a higher concentration of carbon in biochar produced in the batch-operated reactor, but for gorse and broom pyrolysis, the concentration of carbon is slightly higher in the biochar produced in the auger reactor. On the other hand, the biochar produced in the auger reactor shows a lower concentration of oxygen for the conditions tested.

The H/C molar ratio can reflect the graphitization and stability of the biochar, while the O/C value can provide information about the presence of polar functional groups on the surface of the biochar [48]. As shown in Figure 9, for the biochar samples produced, the

H/C molar ratio was in the range of 0.28 to 0.51 and the O/C molar ratio was in the range of 0.08 to 0.22. The higher operating temperatures produce biochars with lower H/C and O/C molar ratios, thus more stable materials. The same behavior was observed by Maoui et al. [56] in the analysis of biochar obtained from two pine wood wastes at pyrolysis temperatures ranging from 500 °C to 700 °C; they reported maximum values of 0.51 and 0.10 for the molar ratios H/C and O/C, respectively, which decreased with increasing temperature. There is a trend for a higher H/C molar ratio in the biochar produced in the auger reactor; the exception is the biochar from gorse, and the O/C molar ratio is always higher in the biochar produced in the batch-operated reactor.

The H/C and O/C molar ratios in the produced biochar are below the guideline maximum values of 0.7 for H/C and 0.4 for O/C stated in the European Biochar Certificate [14], for all conditions tested and for the different biomasses used in this work. Furthermore, the low values of H/C and O/C observed are indicative that the structure of biochar produced has a high chemical stability and consequent resistance to degradation, making it suitable for the same applications as soil amendment and carbon sequestration in soil.

In short, comparing the results obtained for the elemental and ultimate analysis of biochars produced from pyrolysis of four distinct biomass types in the two different scale reactors and at two distinct temperatures, it can be stated that the information obtained in the small-scale batch-operated reactor under the conditions tested can be regarded as a good support to the design of prototypes of continuous-operation reactors, as the auger reactor shown in this work. Also, it was observed that the process temperature has a relevant effect on the properties of the biochar produced in each type of reactor. Higher process temperatures tend to produce a more stable biochar. When the pyrolysis process was carried out at a temperature of 550 °C, the biochar obtained had a higher carbon content and a lower oxygen and hydrogen content compared to the process carried out at 450 °C, resulting in lower O/C and H/C molar ratios at higher temperatures, which indicates a biochar with higher stability.

For the biochar obtained in the auger reactor with continuous operation, a deeper characterization was carried out, including the analysis of its higher heating value, porosity, pH and electrical conductivity, and the concentration of polycyclic aromatic hydrocarbons. Those results are shown in the following sections.

### 3.3.3. Heating Value

Figure 10 shows the HHV for the biochar samples obtained from pyrolysis of the different biomasses in the auger reactor at 450 °C and 550 °C; it is also shown for comparison the HHV of the parent biomass. Additionally, results from other studies for various types of biomasses and their biochars are presented. It is observed that the HHV of biochar is much higher than that of the parent biomass, and increasing the process temperature increases the HHV of the biochar. For the biochar produced from acacia, gorse, broom, and giant reed at 450 °C, the HHV was 23.7, 28.1, 27.6, and 27.6 MJ·kg<sup>-1</sup> (dry material), respectively, and at 550 °C, the HHV was 30.1, 32.6, 29.3, and 29.4 MJ·kg<sup>-1</sup> (dry material), respectively. The LHV values represent about 2% less than the HHV values for all biochar samples, as shown in Figure 11. The biochar from gorse shows always superior HHV and LHV. These heating values support the potential of biochar as suitable for some specific energetic applications. When comparing the results obtained in this study with different biomasses and biochars produced at different temperatures, it is clear that the HHV of biochar is higher than that of the original biomass [2,57,58]. However, for the other studies analyzed, this difference is not as pronounced, which can be related to the carbon content of the materials. Coconut fiber is the biomass with the HHV most similar to that of this study, with approximately 50% wt. carbon content, while the biochar contains around 77% wt. [57]. On the other hand, rice straw shows the greatest difference in HHV, which is also reflected in the carbon concentration: 36% wt. for the biomass and 49% wt. for the biochar [2].

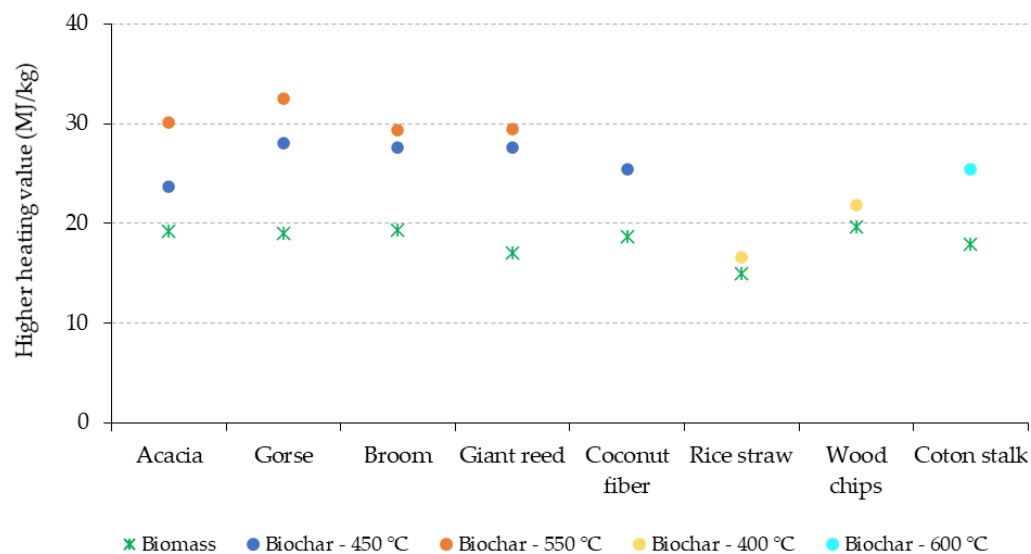


**Figure 10.** Higher heating value (HHV) of the biomass (dry basis) and of the biochar (dry basis) obtained from pyrolysis of the distinct biomasses at 450 °C and 550 °C, and other results from the literature for different biomasses and their biochars [2,57,58].

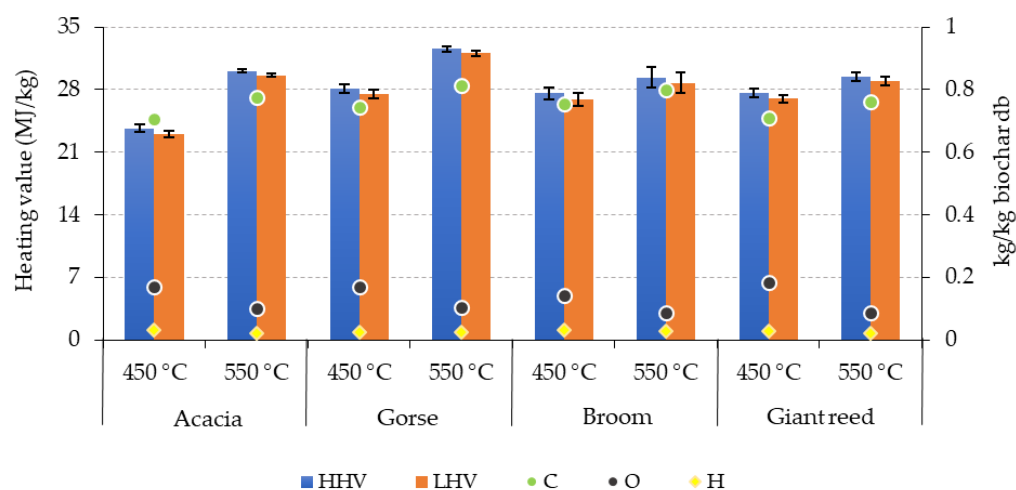


**Figure 11.** Relation between the HHV, LHV, carbon, hydrogen, and oxygen concentrations in the biochar (dry basis) obtained in the pyrolysis of different biomasses in the auger reactor at 450 °C and 550 °C.

The heating value strongly depends on the carbon, hydrogen, and oxygen concentrations in the material. Figure 11 shows the relation between the heating value and the concentration of carbon, hydrogen, and oxygen in the biochar samples. It is observed that the HHV is higher for biochar with a higher carbon concentration and a lower oxygen concentration, as also referred to in other works [59,60]. This can be explained because the heating value of biochar increases with the increase in C–C and C–H bonds on its structure, which releases a higher amount of chemical energy during combustion compared to the O–H and C–O bonds more abundant in biomass [59].

### 3.3.4. pH e Electrical Conductivity

The pH values of the biochar samples obtained from pyrolysis of the different biomasses in the auger reactor at 450 °C and 550 °C are shown in Figure 12. For the biochar obtained from acacia, gorse, broom, and giant reed at 450 °C, the pH was 6.2, 7.5, 6.2, and 8.7, respectively, and at 550 °C, the pH was 7.4, 7.5, 6.9, and 8.8, respectively. There is an increase in the biochar pH with the increase in temperature of the pyrolysis process.

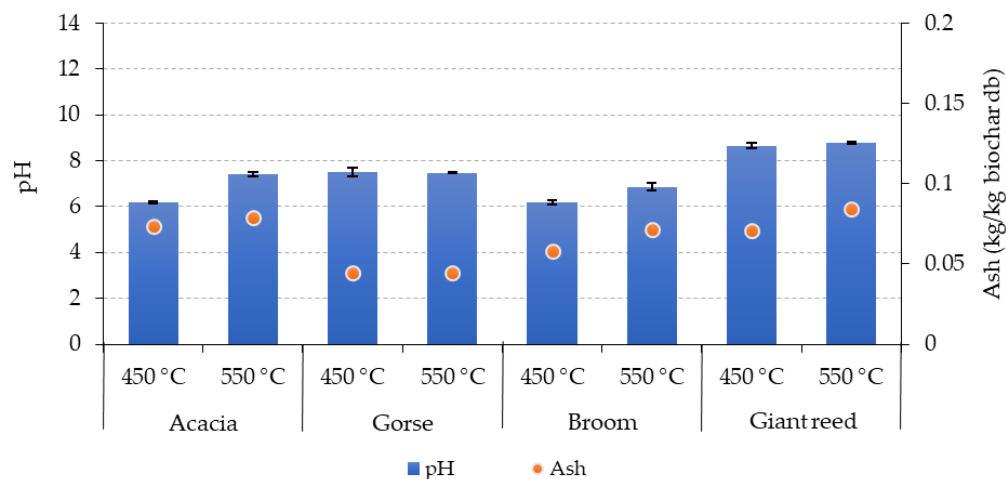


**Figure 12.** pH values and ash concentration for the biochar obtained from pyrolysis of distinct biomasses in the auger reactor at 450 °C and 550 °C.

A direct correlation between the pH of the biochar and its concentration of alkaline elements present in the ashes has been referred to in the literature [50]. This direct correlation is observed for biochars from giant reed, acacia, and broom, with the highest value of pH observed for giant reed, which also has the highest ash concentration. However, the biochar from gorse has the second highest pH value but its ash concentration is the lowest. This behavior can be explained by the composition of the ash from gorse, which can have higher levels of alkaline elements, compared to the ash of biochars obtained from the other biomasses, as also referred to in another study with similar results [50].

The influence of temperature on the biochar pH can be explained as resulting from an increase in the concentration of ash [61] with increasing temperature; in fact, when increasing the pyrolysis temperature, it was observed an increase in the concentration of ash in the biochar (see Figure 8), thus promoting an increase in biochar pH. Other factors can influence the effect of temperature on pH; for example, the increase in concentration of basic functional groups and the disappearance of acidic functional groups with the increase in process temperature have been referred to [62]. This decomposition of acidic functional groups, such as carbonyl, carboxylic, and phenol, is also related to the decrease in the O/C molar ratio that occurs when the pyrolysis temperature is increased [63].

The pH of biochar is relevant considering that one of the most preeminent applications of biochar is its use as a soil conditioner, where the regulation of pH of acidic soils is a main function, but this effect depends on the application rate and the biochar pH value [63]. Morim et al. [64] demonstrated that the pH of soil amended with biochar derived from acacia increased substantially in all treatments compared to the control soil, reaching suitable agronomic values. This increase was directly proportional to the application rate for all particle sizes and pyrolysis temperatures tested, with all factors being statistically significant.

The electrical conductivity of a substrate is related to the amount of soluble salts and is important in the scenario of applying biochar as a soil corrective, as it reflects the capacity of this material as a fertilizer and possible salinization-related issues [50]. In Figure 13 are shown the electrical conductivity values of the produced biochar. The biochar obtained from giant reed has very high electrical conductivity values, ranging from 4500 to 6000  $\mu\text{S}\cdot\text{cm}^{-1}$  for both pyrolysis temperatures. This indicates a high concentration of soluble salts and suggests that its application in the soil can promote salinity problems. For the biochar obtained from other biomass, the electrical conductivity was lower, ranging from 376 to 1540  $\mu\text{S}\cdot\text{cm}^{-1}$ , with biochar from acacia showing the lower value. The increase in the pyrolysis temperature was influenced in order to increase the electrical conductivity for the biochar from acacia, broom, and giant reed, and that can be explained as resulting from the increase in ash concentration with the increase in temperature (see Figure 8). For

the biochar from gorse, the increase in process temperature did not cause the same effect, and the electrical conductivity decreased; again, in this case, as referred about the effect of temperature on pH, the effect of increasing the temperature is related not only with the ash concentration but also with the composition of the ashes and its influence on electrical conductivity. At this stage, it is not possible to go deeper on the subject because there is no available information on the ash composition.

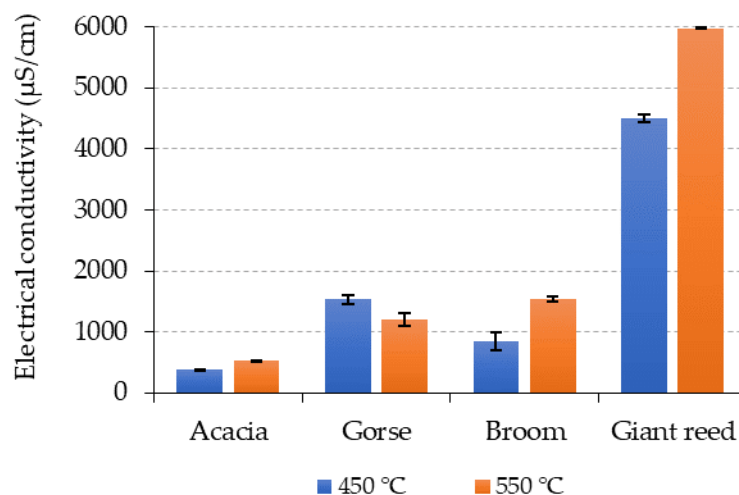


**Figure 13.** Electrical conductivity values for the biochar obtained from pyrolysis of distinct biomasses in the auger reactor at 450 °C and 550 °C.

For comparison purposes, Zhang et al. [65] investigated the influence of pyrolysis temperature on the characteristics of the produced biochar and observed behavior similar to that found in this study. In their analysis, biochars produced from wheat straw, corn straw, rape straw, and rice straw at pyrolysis temperatures ranging from 300 °C to 600 °C were tested, and pH and electrical conductivity values increased with rising temperature. This was attributed to variations in ash content of alkaline minerals, soluble salt content, and acidic functional groups. At higher temperatures (above 500 °C), a slower rate of pH increase was observed.

### 3.3.5. Density and Porosity

It was analyzed density and porosity values for biochar obtained from acacia, gorse, broom, and giant reed, and the results are shown in Figure 14. The bulk density values obtained for all analyzed samples were in the range of 0.09 to 0.15 g·cm<sup>-3</sup> (Figure 14) and are within the range of values referred in the literature for biochar samples, which are from 0.06 to 0.7 g·cm<sup>-3</sup> [50]; the values obtained here are within the lower range of values referred in the literature. The bulk density of the biochar samples did not vary significantly with pyrolysis temperature or type of parent biomass, although a slight decrease with increasing pyrolysis temperature can be observed.

The true density refers only to the density of the solid matrix of the particle and is determined excluding the volume corresponding to the porosity, and its determination requires that a displacement fluid penetrates the pores of the particle. On the other hand, the apparent density considers the total volume of the particle, including the voids (porosity) within the particle. The true density values obtained for the biochar samples ranged from 1.44 to 1.68 g·cm<sup>-3</sup>, while the apparent density ranged from 0.20 to 0.33 g·cm<sup>-3</sup>. Biochar from gorse pyrolysis at both temperatures shows the higher values of apparent density, whereas biochar from giant reed and acacia shows the lower apparent density, although these values are very similar to those of biochar from broom. Biochar from gorse at the lower pyrolysis temperature has also the higher value of true density, whereas the biochar obtained at the higher temperature shows the lower true density. The true density of biochar from acacia, broom, and giant reed is very similar, and for the range of pyrolysis

temperature used (450 °C and 550 °C). Although a decrease in true density is observed with increasing temperature for biochar from gorse, on the other hand, the effect temperature on this property for biochar from acacia, broom, and giant reed seems not to be relevant.

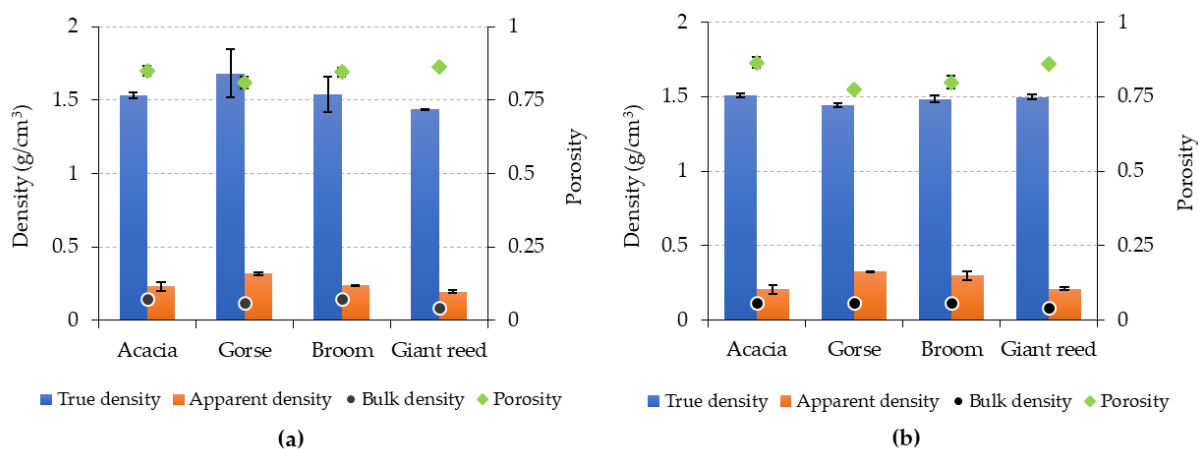


**Figure 14.** Porosity and true, apparent, and bulk density of the biochar from pyrolysis of distinct biomasses in the auger reactor at (a) 450 °C and (b) 550 °C.

High porosity values, from 0.77 to 0.86 (Figure 14), were found in the biochar samples produced in this work from pyrolysis of different biomasses at pyrolysis temperatures of 450 °C and 550 °C; the porosity was determined through the relationship between the true density and the apparent density. Biochar from giant reed and acacia shows the highest porosity values, whereas biochar from gorse shows the lowest porosity values. For acacia, the maximum value was observed in biochar produced at the higher pyrolysis temperature. Some studies report an increase in the porosity of the biochar when the pyrolysis temperature is increased, explained by the formation of voids due to the higher release of volatile compounds at higher temperatures [50,66]. In this work, that trend is observed for biochar from acacia but not for the biochar from gorse or broom, where a slight decrease in porosity was observed with increasing temperature. For biochar from giant reed, no significant difference in porosity was observed as a function of pyrolysis temperature. Several factors can explain this distinct effect of temperature on the porosity of biochar from distinct feedstocks, namely, variables such as the chemical composition, ash, and organic carbon content of the parent biomass [67]. The porosity of biochar is a relevant physical property, namely, but not only, on its behavior as an additive in soils, for example, as it can affect the water holding capacity, cation exchange capacity, and adsorption capacity.

### 3.3.6. Polycyclic Aromatic Hydrocarbons and Polychlorinated Biphenyls

During the pyrolysis of biomass, complex aromatic structures are formed, which range in size from a simple ring to large sheets of graphene. Among these organic compounds are the polycyclic aromatic hydrocarbons (PAHs), which have complex formation mechanisms [68,69]. Although most PAHs, which are lighter molecules, are in the gas or liquid phase, some residual molecules may remain adsorbed in the biochar. In addition to the pyrolysis conditions (e.g., temperature) that influence the concentration of PAHs in biochar, other factors can influence that concentration, for example, cooling of biochar in the presence of pyrolysis volatiles [14,70]. The concentration of PAHs in biochar is extremely important due to the potential environmental hazards, including the carcinogenic and mutagenic effects of these compounds on human health [71]. Polychlorinated biphenyl compounds (PCBs) belong to a family of halogenated aromatic hydrocarbons that are generally present in minimum amounts in biochar, and their concentration depends on the chlorine concentration present in the parent biomass, which for most biomass types is usually very low.

The effect of pyrolysis temperature on the concentration of PAHs in biochar is still not well established in the literature [69]. However, some studies indicate that a moderate pyrolysis temperature (400–550 °C) produces higher concentrations of PAHs in biochar [71,72]. In this work, the PAHs and PCBs concentrations were analyzed in the biochar obtained from pyrolysis of acacia, gorse, broom, and giant reed in an auger reactor at 450 °C and 550 °C with 5 min of residence time.

Table 4 shows the concentration of PAHs and PCBs in the biochar samples, as well as their maximum concentration limits established by the European Biochar Certificate [14]. The reported concentration value for PAHs comprises the sum of sixteen priority compounds, which are acenaphthene(b), acenaphthylene, anthracene, benzo(a)anthracene, benzo(a)pyrene, benzo(b)fluoranthene, benzo(g,h,i)perylene, benzo(k)fluoranthene, chrysene, dibenzo(a,h)anthracene, phenanthrene, fluoranthene, fluorene, indeno(1,2,3-c,d)pyrene, naphthalene, and pyrene, and for PCBs the concentration is the sum of seven compounds (PCB 101, PCB 118, PCB 138, PCB 153, PCB 180, PCB 28, and PCB 52).

**Table 4.** PAHs and PCBs concentration (in  $\text{mg}\cdot\text{kg}^{-1}$ ) present in the biochar samples from pyrolysis of distinct biomasses in the auger reactor at 450 °C and 550 °C with 5 min of residence time.

	Maximum Value *	Temperature (°C)	Acacia	Gorse	Broom	Giant Reed
PAHs	$6 \pm 2.4$	450	0.13	0.21	2.64	<0.12
		550	<0.12	<0.13	<0.13	<0.14
PCBs	0.2	450	<0.02	<0.02	<0.02	<0.12
		550	<0.12	<0.13	<0.13	<0.14

\* Maximum concentration value defined by EBC [14].

It was observed that the PAH and PCB concentration values obtained for the tested biochar samples are well below the maximum concentration limit indicated by the European Biochar Certificate [14] for materials to be applied in the soil. These results are indicative of suitable and satisfactory pyrolysis process conditions used for the production of biochar in the auger reactor.

#### 4. Conclusions

The results obtained in this work show that, according to the analyzed properties, the pyrolysis of residual forest biomass from acacia, gorse, broom, and giant reed produces a biochar with suitable characteristics for several applications, such as, for example, an additive to improve soil properties. The concentration of carbon, PAHs and PCBs content, and O/C and H/C molar ratios were obtained for the biochar fall within the guidelines indicated in the European Biochar Certificate.

The characteristics of the biochar obtained are influenced by the type of biomass and operational conditions of the process, and the pyrolysis temperature is a parameter that has a relevant effect on the biochar characteristics. The results indicate that biochar obtained at 550 °C has a higher yield and a higher concentration of volatiles, oxygen, and hydrogen, but lower ash content, heating value, and carbon content compared to the biochar obtained at 450 °C.

When analyzing the change in reactor type and scale, it can be concluded that the yield and properties of biochar produced in the small-scale fixed-bed batch-operated reactor can be used as a good approach to estimate the yield and properties expected in biochar produced in higher-scale and continuous-operation reactors as the prototype of auger reactor used in this work. However, it is important to state that some differences can be noticed; for example, the biochar yield in the auger reactor was slightly lower than in the fixed-bed batch reactor. Nevertheless, obtaining similar biochar yield and characteristics in both types of reactors and scales is a promising aspect in the scenario of using this approach as a good supporting tool for scaling up technology and thus to valorize low-grade residual biomass from forest management activities for wildfire prevention.

Future studies will focus on evaluating the potential thermal energy available in the pyrolysis process to develop autothermal reactors, where the energy from the combustion of pyrolysis vapors is utilized to sustain the process thermally. Advancing toward autothermal processes is crucial for enabling the use of pyrolysis reactors on an even larger processing scale for biochar production from biomass.

**Author Contributions:** Conceptualization, M.S. and L.A.C.T.; methodology, M.S. and L.A.C.T.; investigation, M.S., A.C.M., M.V. and L.A.C.T.; writing—original draft preparation, M.S.; resources, M.S. and L.A.C.T.; writing—review and editing, F.S., M.M. and L.A.C.T.; supervision, L.A.C.T.; project administration, L.A.C.T. All authors have read and agreed to the published version of the manuscript.

**Funding:** This research was performed in the scope of the Project BioValChar—Sustainable valorisation of residual biomass for biochar, PCIF-GVB-0034-2019, <http://doi.org/10.54499/PCIF/GVB/0034/2019>, funded by the Portuguese Foundation for Science and Technology (FCT). Acknowledgment also to the Project InPacTus—Innovative products and technologies from eucalyptus, POCI-01-0247-FEDER-021874, funded by Portugal 2020 through the European Regional Development Fund (ERDF) in the frame of the COMPETE 2020 n°246/AXIS II/2017. Thanks are due to the Portuguese Foundation for Science and Technology (FCT)/Ministry of Science, Technology and Higher Education (MCTES), Portugal, for their financial support to CESAM (UIDP/50017/2020+UIDB/50017/2020+LA/P/0094/2020) through national funds.

**Data Availability Statement:** Data are contained within the article.

**Conflicts of Interest:** The authors declare no conflicts of interest.

## References

- Jacinto, G.S.S.; Cruz, G.; Cabral, A.A.; Bezerra, G.V.P.; Garcia, R.R.P.; Magalhães, U.N.; Gomes, W.C. Biotechnological investigation of *Pediastrum boryanum* and *Desmodesmus subspicatus* microalgae species for a potential application in bioenergy. *Algal Res.* **2023**, *75*, 105881. [[CrossRef](#)]
- Anand, A.; Gautam, S.; Ram, L.C. Feedstock and pyrolysis conditions affect suitability of biochar for various sustainable energy and environmental applications. *J. Anal. Appl. Pyrolysis* **2023**, *170*, 105881. [[CrossRef](#)]
- Cruz, G.; Crnkovic, P.M. Assessment of the physical–chemical properties of residues and emissions generated by biomass combustion under N<sub>2</sub>/O<sub>2</sub> and CO<sub>2</sub>/O<sub>2</sub> atmospheres in a Drop Tube Furnace (DTF). *J. Therm. Anal. Calorim.* **2019**, *138*, 401–415. [[CrossRef](#)]
- Briones-Hidrovo, A.; Copa, J.; Tarelho, L.A.; Gonçalves, C.; da Costa, T.P.; Dias, A.C. Environmental and energy performance of residual forest biomass for electricity generation: Gasification vs. combustion. *J. Clean. Prod.* **2021**, *289*, 125680. [[CrossRef](#)]
- Enes, T.; Aranha, J.; Fonseca, T.; Lopes, D.; Alves, A.; Lousada, J. Thermal Properties of Residual Agroforestry Biomass of Northern Portugal. *Energies* **2019**, *12*, 1418. [[CrossRef](#)]
- Guerra-Hernández, J.; Pereira, J.M.; Stovall, A.; Pascual, A. Impact of fire severity on forest structure and biomass stocks using NASA GEDI data. Insights from the 2020 and 2021 wildfire season in Spain and Portugal. *Sci. Remote Sens.* **2024**, *9*, 100134. [[CrossRef](#)]
- Instituto Da Conservação Da Natureza E Das Florestas-SGIF/Sistema de Gestão de Instituto de Incêndios Florestas-Relatório Provisório de Incêndios Rurais. Available online: <https://www.icnf.pt/> (accessed on 15 July 2024).
- EFFIS—European Forest Fire Information System—Forest Fires in Europe, Middle East and North Africa 2022. Available online: <https://forest-fire.emergency.copernicus.eu> (accessed on 14 July 2024).
- Amjith, L.; Bavanish, B. A review on biomass and wind as renewable energy for sustainable environment. *Chemosphere* **2022**, *293*, 133579. [[CrossRef](#)]
- Niu, Y.; Tan, H.; Hui, S. Ash-related issues during biomass combustion: Alkali-induced slagging, silicate melt-induced slagging (ash fusion), agglomeration, corrosion, ash utilization, and related countermeasures. *Prog. Energy Combust. Sci.* **2016**, *52*, 1–61. [[CrossRef](#)]
- Koppejan, J.; van Loo, S. *The Handbook of Biomass Combustion and Co-Firing*, 1st ed.; Routledge: London, UK, 2007.
- Neves, D.; Matos, A.; Tarelho, L.; Thunman, H.; Larsson, A.; Seemann, M. Volatile gases from biomass pyrolysis under conditions relevant for fluidized bed gasifiers. *J. Anal. Appl. Pyrolysis* **2017**, *127*, 57–67. [[CrossRef](#)]
- Neves, D.; Thunman, H.; Matos, A.; Tarelho, L.; Gómez-Barea, A. Characterization and prediction of biomass pyrolysis products. *Prog. Energy Combust. Sci.* **2011**, *37*, 611–630. [[CrossRef](#)]
- European Biochar Foundation. European Biochar Certificate—Guidelines for a Sustainable Production of Biochar. Volume 10.1. Available online: <http://european-biochar.org> (accessed on 15 July 2024).
- Silva, F.C.; Santos, M.; Moura, J.; Boas, A.C.V.; Matos, M.A.; Tarelho, L.A.C. Preventing wildfires through smart management and valorisation of residual forest biomass into biochar: Experiences from the BioValChar project. In *Advances in Forest Fire Research*; Imprensa da Universidade de Coimbra: Coimbra, Portugal, 2022; pp. 1507–1512. [[CrossRef](#)]

16. Verheijen, F.G.A.; Zhuravel, A.; Silva, F.C.; Amaro, A.; Ben-Hur, M.; Keizer, J.J. The influence of biochar particle size and concentration on bulk density and maximum water holding capacity of sandy vs sandy loam soil in a column experiment. *Geoderma* **2019**, *347*, 194–202. [[CrossRef](#)]
17. Muigai, H.H.; Bordoloi, U.; Hussain, R.; Ravi, K.; Moholkar, V.S.; Kalita, P. A comparative study on synthesis and characterization of biochars derived from lignocellulosic biomass for their candidacy in agronomy and energy applications. *Int. J. Energy Res.* **2020**, *45*, 4765–4781. [[CrossRef](#)]
18. Amen, R.; Yaseen, M.; Mukhtar, A.; Klemeš, J.J.; Saqib, S.; Ullah, S.; Al-Sehemi, A.G.; Rafiq, S.; Babar, M.; Fatt, C.L.; et al. Lead and cadmium removal from wastewater using eco-friendly biochar adsorbent derived from rice husk, wheat straw, and corncob. *Clean. Eng. Technol.* **2020**, *1*, 100006. [[CrossRef](#)]
19. Hairuddin, M.N.; Mubarak, N.M.; Khalid, M.; Abdullah, E.C.; Walvekar, R.; Karri, R.R. Magnetic palm kernel biochar potential route for phenol removal from wastewater. *Environ. Sci. Pollut. Res.* **2019**, *26*, 35183–35197. [[CrossRef](#)] [[PubMed](#)]
20. Javanmard, A.; Zuki, F.M.; Patah, M.F.A.; Daud, W.M.A.W. Revolutionizing microbial fuel cells: Biochar's energy conversion odyssey. *Process. Saf. Environ. Prot.* **2024**, *187*, 26–58. [[CrossRef](#)]
21. Tsarpali, M.; Kuhn, J.N.; Philippidis, G.P.; Tsarpali, M.; Kuhn, J.N.; Philippidis, G.P. Activated carbon production from algal biochar: Chemical activation and feasibility analysis. *Fuel Commun.* **2024**, *19*, 100115. [[CrossRef](#)]
22. Singh, S.; Bhaumik, S.K.; Dong, L.; Vuthaluru, H. Enhanced tar removal in syngas cleaning through integrated steam catalytic tar reforming and adsorption using biochar. *Fuel* **2023**, *331*, 125912. [[CrossRef](#)]
23. Kusuma, H.S.; Az-Zahra, K.D.; Saputri, R.W.; Utomo, M.D.P.; Jaya, D.E.C.; Amenaghawon, A.N.; Darmokoesoemo, H. Unlocking the potential of agricultural waste as biochar for sustainable biodiesel production: A comprehensive review. *Bioresour. Technol. Rep.* **2024**, *26*, 101848. [[CrossRef](#)]
24. Yadav, K.; Tyagi, M.; Kumari, S.; Jagadevan, S. Influence of Process Parameters on Optimization of Biochar Fuel Characteristics Derived from Rice Husk: A Promising Alternative Solid Fuel. *BioEnergy Res.* **2019**, *12*, 1052–1065. [[CrossRef](#)]
25. del Pozo, C.; Rego, F.; Puy, N.; Bartolí, J.; Fàbregas, E.; Yang, Y.; Bridgwater, A.V. The effect of reactor scale on biochars and pyrolysis liquids from slow pyrolysis of coffee silverskin, grape pomace and olive mill waste, in auger reactors. *Waste Manag.* **2022**, *148*, 106–116. [[CrossRef](#)]
26. Miranda Santos, S.D.F.d.O.; Piekarski, C.M.; Ugaya, C.M.L.; Donato, D.B.; Júnior, A.B.; De Francisco, A.C.; Carvalho, A.M.M.L. Life cycle analysis of charcoal production in masonry kilns with and without carbonization process generated gas combustion. *Sustainability* **2017**, *9*, 1558. [[CrossRef](#)]
27. Salgado MA, H.; Tarelho, L.A. Simultaneous production of biochar and thermal energy using palm oil residual biomass as feedstock in an auto-thermal prototype reactor. *J. Clean. Prod.* **2020**, *266*, 121804. [[CrossRef](#)]
28. Gómez, N.; Rosas, J.G.; Cara, J.; Martínez, O.; Albuquerque, J.A.; Sánchez, M.E. Slow pyrolysis of relevant biomasses in the Mediterranean basin. Part 1. Effect of temperature on process performance on a pilot scale. *J. Clean. Prod.* **2016**, *120*, 181–190. [[CrossRef](#)]
29. Brassard, P.; Godbout, S.; Raghavan, V. Pyrolysis in auger reactors for biochar and bio-oil production: A review. *Biosyst. Eng.* **2017**, *161*, 80–92. [[CrossRef](#)]
30. Campuzano, F.; Brown, R.C.; Martínez, J.D. Auger reactors for pyrolysis of biomass and wastes. *Renew. Sustain. Energy Rev.* **2019**, *102*, 372–409. [[CrossRef](#)]
31. Meng, J.; Zhang, H.; Cui, Z.; Guo, H.; Mašek, O.; Sarkar, B.; Wang, H.; Bolan, N.; Shan, S. Comparative study on the characteristics and environmental risk of potentially toxic elements in biochar obtained via pyrolysis of swine manure at lab and pilot scales. *Sci. Total. Environ.* **2022**, *825*, 153941. [[CrossRef](#)]
32. Prithiraj, S.; Kauchali, S. Yields from pyrolysis of refinery residue using a batch process. *S. Afr. J. Chem. Eng.* **2017**, *24*, 95–115. [[CrossRef](#)]
33. Park, K.B.; Chae, D.Y.; Fini, E.H.; Kim, J.S. Pyrolysis of biomass harvested from heavy-metal contaminated area: Characteristics of bio-oils and biochars from batch-wise one-stage and continuous two-stage pyrolysis. *Chemosphere* **2024**, *355*, 141715. [[CrossRef](#)]
34. CEN/TS 14774-3:2004; Solid Biofuels—Methods for the Determination of Moisture Content. European Committee for Standardization: Brussels, Belgium, 2004.
35. CEN/TS 15148:2005; Solid Biofuels—Method for the Determination of the Content of Volatile Matter. European Committee for Standardization: Brussels, Belgium, 2005.
36. CEN/TS 14775:2004; Solid Biofuels—Method for the Determination of Ash Content. European Committee for Standardization: Brussels, Belgium, 2004.
37. DIN 51900; Determining the Gross Calorific Value of Solid and Liquid Fuels Using the Bomb Calorimeter, and Calculation of Net Calorific Value. Deutsches Institut für Normung: Berlin, Germany, 2000.
38. SIS-CEN/TS 15103:2006; Solid Biofuels—Methods for the Determination of Bulk Density. European Committee for Standardization: Brussels, Belgium, 2006.
39. ISO 10390:2021; Soil, Treated Biowaste and Sludge—Determination of pH. International Organization for Standardization: Geneva, Switzerland, 2021.
40. ISO 11265:1994; Soil Quality—Determination of the Specific Electrical Conductivity. International Organization for Standardization: Geneva, Switzerland, 1994.

41. Matos, M.A.A. Formação e redução de NO<sub>x</sub> na combustão de coque em leito fluidizado. Ph.D. Thesis, University of Aveiro, Aveiro, Portugal, September 1995.
42. ASTM. Gaseous Fuels; Coal and Coke. In *Annual Book of ASTM Standards—Section 5—Petroleum Products, Lubricants, and Fossil Fuels*; American Society for Testing and Materials: Philadelphia, PA, USA, 1991; Volume 05.05.
43. ASTM. Refractories, Glass, Ceramic Materials; Carbon and Graphite Products. In *Annual Book of ASTM Standards—Part 17*; American Society for Testing and Materials: Easton, PA, USA, 1981.
44. Perch, M. Solid products of pyrolysis. In *Chemistry of Coal Utilization: Second Supplementary Volume*; Elliot, M.A., Ed.; John Wiley & Sons Inc.: New York, NY, USA, 1981.
45. Sharkey, A.G. Physical properties of coals and its products. In *Chemistry of Coal Utilization: Second Supplementary Volume*; Elliot, M.A., Ed.; John Wiley & Sons Inc.: New York, NY, USA, 1981.
46. ISO 18287:2006; Soil Quality—Determination of Polycyclic Aromatic Hydrocarbons (PAH)—Gas Chromatographic Method with Mass Spectrometric Detection (GC-MS). International Organization for Standardization: Geneva, Switzerland, 2006.
47. ISO 18475:2023; Environmental Solid Matrices—Determination of Polychlorinated Biphenyls (PCB) by Gas Chromatography—Mass Selective Detection (GC-MS) or Electron-Capture Detection (GC-ECD). International Organization for Standardization: Geneva, Switzerland, 2023.
48. Tan, Z.; Lin, C.S.; Ji, X.; Rainey, T.J. Returning biochar to fields: A review. *Appl. Soil Ecol.* **2017**, *116*, 1–11. [[CrossRef](#)]
49. de Paula Protásio, T.; Bufalino, L.; Tonoli, G.H.D.; Couto, A.M.; Trugilho, P.F.; Júnior, M.G. Relação entre o poder calorífico superior e os componentes elementares e minerais da biomassa vegetal. *Pesqui. Florest. Bras.* **2011**, *31*, 113–122. [[CrossRef](#)]
50. Balmuk, G.; Videgain, M.; Manyà, J.J.; Duman, G.; Yanik, J. Effects of pyrolysis temperature and pressure on agronomic properties of biochar. *J. Anal. Appl. Pyrolysis* **2023**, *169*, 105858. [[CrossRef](#)]
51. Lin, B.J.; Silveira, E.A.; Colin, B.; Chen, W.H.; Lin, Y.Y.; Leconte, F.; Pétrissans, A.; Rousset, P.; Pétrissans, M. Modeling and prediction of devolatilization and elemental composition of wood during mild pyrolysis in a pilot-scale reactor. *Ind. Crop. Prod.* **2019**, *131*, 357–370. [[CrossRef](#)]
52. Silveira, E.A.; Lin, B.J.; Colin, B.; Chaouch, M.; Pétrissans, A.; Rousset, P.; Chen, W.-H.; Pétrissans, M. Heat treatment kinetics using three-stage approach for sustainable wood material production. *Ind. Crop. Prod.* **2018**, *124*, 563–571. [[CrossRef](#)]
53. Yang, Y.; Qian, X.; Alamu, S.O.; Brown, K.; Lee, S.W.; Kang, D.H. Qualities and Quantities of Poultry Litter Biochar Characterization and Investigation. *Energies* **2024**, *17*, 2885. [[CrossRef](#)]
54. Qian, C.; Li, Q.; Zhang, Z.; Wang, X.; Hu, J.; Cao, W. Prediction of higher heating values of biochar from proximate and ultimate analysis. *Fuel* **2020**, *265*, 116925. [[CrossRef](#)]
55. Toczydlowski, A.J.; Slesak, R.A.; Venterea, R.T.; Spokas, K.A. Pyrolysis temperature has greater effects on carbon and nitrogen biogeochemistry than biochar feedstock when applied to a sandy forest soil. *For. Ecol. Manag.* **2023**, *534*, 120881. [[CrossRef](#)]
56. Maaoui, A.; Trabelsi, A.B.H.; Ben Abdallah, A.; Chaghtmi, R.; Lopez, G.; Cortazar, M.; Olazar, M. Assessment of pine wood biomass wastes valorization by pyrolysis with focus on fast pyrolysis biochar production. *J. Energy Inst.* **2023**, *108*, 101242. [[CrossRef](#)]
57. Dhar, S.A.; Sakib, T.U.; Hilary, L.N. Effects of pyrolysis temperature on production and physicochemical characterization of biochar derived from coconut fiber biomass through slow pyrolysis process. *Biomass-Convert. Biorefin.* **2020**, *12*, 2631–2647. [[CrossRef](#)]
58. He, X.; Liu, Z.; Niu, W.; Yang, L.; Zhou, T.; Qin, D.; Niu, Z.; Yuan, Q. Effects of pyrolysis temperature on the physicochemical properties of gas and biochar obtained from pyrolysis of crop residues. *Energy* **2018**, *143*, 746–756. [[CrossRef](#)]
59. Kongto, P.; Palamanit, A.; Ninduangdee, P.; Singh, Y.; Chanakaewsomboon, I.; Hayat, A.; Wae-Hayee, M. Intensive exploration of the fuel characteristics of biomass and biochar from oil palm trunk and oil palm fronds for supporting increasing demand of solid biofuels in Thailand. *Energy Rep.* **2022**, *8*, 5640–5652. [[CrossRef](#)]
60. Xie, T.; Yao, Z.; Huo, L.; Jia, J.; Zhang, P.; Tian, L.; Zhao, L. Characteristics of biochar derived from the co-pyrolysis of corn stalk and mulch film waste. *Energy* **2023**, *262*, 125554. [[CrossRef](#)]
61. Tomczyk, A.; Sokołowska, Z.; Boguta, P. Biochar physicochemical properties: Pyrolysis temperature and feedstock kind effects. *Rev. Environ. Sci. Bio/Technol.* **2020**, *19*, 191–215. [[CrossRef](#)]
62. Al-Wabel, M.I.; Al-Omran, A.; El-Naggar, A.H.; Nadeem, M.; Usman, A.R. Pyrolysis temperature induced changes in characteristics and chemical composition of biochar produced from conocarpus wastes. *Bioresour. Technol.* **2013**, *131*, 374–379. [[CrossRef](#)] [[PubMed](#)]
63. Hass, A.; Gonzalez, J.M.; Lima, I.M.; Godwin, H.W.; Halvorson, J.J.; Boyer, D.G. Chicken Manure Biochar as Liming and Nutrient Source for Acid Appalachian Soil. *J. Environ. Qual.* **2012**, *41*, 1096–1106. [[CrossRef](#)]
64. Morim, A.C.; dos Santos, M.C.; Tarelho, L.A.C.; Silva, F.C. Physicochemical Improvements in Sandy Soils through the Valorization of Biomass into Biochar. *Energies* **2023**, *16*, 7645. [[CrossRef](#)]
65. Zhang, X.; Zhang, P.; Yuan, X.; Li, Y.; Han, L. Effect of pyrolysis temperature and correlation analysis on the yield and physicochemical properties of crop residue biochar. *Bioresour. Technol.* **2019**, *296*, 122318. [[CrossRef](#)]
66. Luo, L.; Xu, C.; Chen, Z.; Zhang, S. Properties of biomass-derived biochars: Combined effects of operating conditions and biomass types. *Bioresour. Technol.* **2015**, *192*, 83–89. [[CrossRef](#)]
67. Leng, L.; Xiong, Q.; Yang, L.; Li, H.; Zhou, Y.; Zhang, W.; Jiang, S.; Li, H.; Huang, H. An overview on engineering the surface area and porosity of biochar. *Sci. Total. Environ.* **2020**, *763*, 144204. [[CrossRef](#)]

68. Mengesha, T.T.; Ancha, V.R.; Sundar, L.S.; Pollex, A. Review on the Influence of Pyrolysis Process Parameters for Biochar Production with Minimized Polycyclic Aromatic Hydrocarbon Content. *J. Anal. Appl. Pyrolysis* **2024**, *182*, 106699. [[CrossRef](#)]
69. Wang, C.; Wang, Y.; Herath, H. Polycyclic aromatic hydrocarbons (PAHs) in biochar—Their formation, occurrence and analysis: A review. *Org. Geochem.* **2017**, *114*, 1–11. [[CrossRef](#)]
70. Laird, D.A.; Brown, R.C.; Amonette, J.E.; Lehmann, J. Review of the pyrolysis platform for coproducing bio-oil and biochar. *Biofuels Bioprod. Biorefin.* **2009**, *3*, 547–562. [[CrossRef](#)]
71. Devi, P.; Dalai, A.K. Occurrence, distribution, and toxicity assessment of polycyclic aromatic hydrocarbons in biochar, biocrude, and biogas obtained from pyrolysis of agricultural residues. *Bioresour. Technol.* **2023**, *384*, 129293. [[CrossRef](#)] [[PubMed](#)]
72. Devi, P.; Saroha, A.K. Effect of pyrolysis temperature on polycyclic aromatic hydrocarbons toxicity and sorption behaviour of biochars prepared by pyrolysis of paper mill effluent treatment plant sludge. *Bioresour. Technol.* **2015**, *192*, 312–320. [[CrossRef](#)] [[PubMed](#)]

**Disclaimer/Publisher’s Note:** The statements, opinions and data contained in all publications are solely those of the individual author(s) and contributor(s) and not of MDPI and/or the editor(s). MDPI and/or the editor(s) disclaim responsibility for any injury to people or property resulting from any ideas, methods, instructions or products referred to in the content.